

Analysis of Rural Health Prediction Machine Learning Algorithms with LSTM-GAN Architecture for 5G Medical Time-Series Analysis

Diksha Dalal¹, Dr. Ankit Kumar², Dr. Sandeep Kumar³

¹Research Scholar, Baba Mastnath University, Asthal Bohar, Rohtak

²Assistant Professor, Baba Mastnath University, Asthal Bohar, Rohtak

³Associate Professor, Maharaja Surajmal Institute of Technology, Janakpuri, New Delhi

Abstract:

For smart health-care services and apps, 4G and other communication standards are employed in the healthcare industry. These technologies are essential to the development of smart healthcare services in the future. As the health care sector expands, several applications are anticipated to generate enormous amounts of data in various formats and sizes. Such vast and varied data requires specific handling with regard to end-to-end delay, bandwidth, latency, and other factors. Information and communication technology is developing quickly today. The system must be created in such a way that it takes into account the preferences of senior people, who have additional needs in terms of their living arrangements and the environment in which they live. In order to examine the most important criteria (feature) needed to develop a model for spotting strange behavior in elderly people, this study recommended using the "Decision Making Trial and Evaluation Laboratory" (DEMATEL). After DEMATEL analyzed the main criteria for predicting odd behavior in the elderly, Convolutional Neural Networks (CNNs) and Long Short-Term Memories (LSTMs) were adopted in the detection of strange behavior in the elderly. The study developed a theory by relating the SIMADL dataset to the behavior of elderly persons and then carried out an experimental investigation with CNN and LSTM-GAN. According to performance assessments, the LSTM has a 97% accuracy rate when it comes to identifying odd behavior in elderly people.

Keywords: IoT, Machine Learning Approaches, Electronic Health Records, 5G Network, CNN.

1. INTRODUCTION

Although the healthcare sector has been increasingly digitalized, the anticipated effects of the Internet on healthcare have not yet materialized. The potential contributing elements include an increase in patient participation, connected care, irrisistant patient monitoring, and assisted living for elderly and chronically ill patients. When consumers need e-prescriptions, which allow doctors to dispense medicines over the phone or via email, and emedicine, which allows pharmaceutical companies to transport medications directly to patients' homes, this sort of healthcare is advantageous. The world at this time is made up entirely of people who are becoming older. According to a WHO status report [1], the total world population over 65 years old was 702.9 million in 2019 and is expected to increase by 120% to about 1549 million by the year 2050. Similarly, the number of adults 80 years and older was approximately 53.9 million in 2019 and is projected to increase to 109.1 million by the year 2050, representing a total increase of 102.6%. An estimated 50 million people worldwide suffer from dementia as of 2019, and that number is expected to rise to 150 million by the year 2050. Of all these patients, 80% fall into the 75–95 age range. Over 70% of these patients will be reliant on the caregivers for their everyday tasks. To reverse the cognitive limits of the sick group, there is, however, no feasible alternative.

The healthcare sector is seeing rapid growth and market expansion, as well as a significant increase in the number of applications that will benefit from employing an Internet-like network. The diverse data types, sizes, and formats produced by this sector place significant demands on the network in terms of network bandwidth, latency, data rate, and a number of other variables. The eHealthcare service starts with the deployment of sensor equipment in various locations around the healthcare facilities, which will afterwards link to the network via networking technologies like Wi-Fi, Bluetooth, and other related technologies. As eHealthcare develops, connecting technologies should also advance because large eHealthcare facilities will need a significant number of sensors and other types of equipment to run multiple sensing applications at once, which will lead to an increase in mMTC. The following in the sequence is cMTC/URLLC [2], which is very beneficial for robotic remote surgeries over tactile Internet.

Because it can collect data by sensing items and communicating with other devices over wireless networks, the Internet of Things (IoT) has become extremely popular. IoT devices can sense, visualize, collect, and share data, and they can

communicate with one another via wireless IoT protocols including Bluetooth, ZigBee, Z-Wave, WiFi, and RFID [3–4]. These protocols are essential to the healthcare industry since they allow for simple data monitoring and communication among the used equipment. These devices' collected data are utilized for a variety of functions, including disease classification, designing, patient monitoring, and other things. This scenario can be managed by new emerging technology, namely, tiny wireless chips or sensors connected with IoT devices remotely monitoring patient's health [5]. In remote places where one cannot reach the hospital services, suffers much, and this results in the patient condition getting worse. It facilitates decision-making when wired or wireless sensors [6] attached to the patient's body safely collect patient data while also giving doctors access to the data. Everyone benefits from IoT applications in the healthcare sector since they allow for remote access to medical assistance, an extension of the length of therapy, and low cost. Numerous studies have used various smart health devices, such as automated insulin delivery (AID) systems, remote care biometric scanners, smart thermometers, sleep monitors, drug interaction monitors, and so on.

Smart healthcare systems also greatly benefit from the use of cloud principles. Data can be accessed securely and effectively, stored efficiently, and the aforementioned problems can be solved by using cloud services. Convolutional neural networks (CNN), autoencoders (AE), deep belief networks (DBNs), long short-term memory (LSTM), recurrent neural networks (RNNs), and other deep learning (DL) approaches are being used to evaluate enormous amounts of data and to accurately detect and diagnose a variety of diseases [8, 9]. Applications of DL in medical signals and imaging benefit patients and doctors alike. Smart healthcare services are greatly improved when IoT technologies are combined with cloud services, machine learning, and deep learning approaches [10].

1.1 Application of GAN in Medical Informatics

Electronic medical records (EMR) have exploded in popularity due to the development of health information technology, hospital information systems, Internet of Things (IoT)-based health platforms, wearable technology, and other platforms (83). The application of scientific research and algorithms in medicine has also been made easier by the expansion in the quantity and quality of medical data. Although patient data can be deidentified, due to data security, particularly privacy protection, the medical data after de-identification can still be reidentified by some combinations. Because of these hurdles, it is exceedingly challenging to connect medical data gathered from various media, which reduces the amount of medical data available for scientific research. Medical informatics applications frequently need a lot of data to train their parameters. The use of deep learning algorithms, particularly artificial intelligence in the field of medical informatics, is severely constrained by the paucity of medical data. Consequently, the advancement of medical informatics lags behind disciplines like medical imaging.

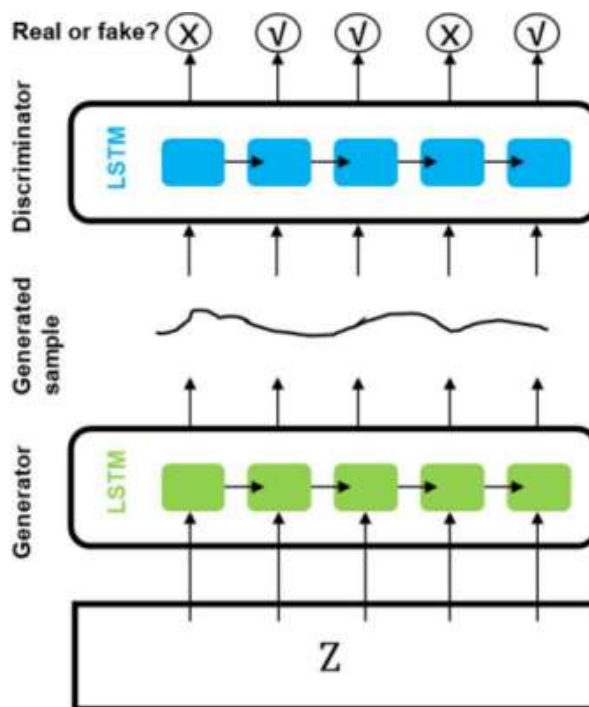


Figure 1: The architecture of LSTM-based GAN in Health Prediction

The fabricated electronic health records (EHR) based on datasets from the Sutter Palo Alto Medical Foundation (PAMF) and the Medical Information Mart for Intensive Care (MIMIC-III) using medical Generative Adversarial Networks (medGAN). The patient's discrete data cannot be directly learned using the original GAN. By utilizing the

autoencoder, medGAN can handle highdimensional multi-label discrete variables (binary and count variables such as diagnoses, drugs, and procedure codes) and get over the original GAN's restriction. The autoencoder picked up information from actual patient records, and the autoencoder's decoder was also employed to create the discrete output after the generator. Impressive findings for discrete variables were obtained.

Modern healthcare difficulties must be addressed with the use of cutting-edge technologies, especially in rural areas where access to expert medical treatment is frequently restricted. The combination of machine learning algorithms and the fast connectivity of 5G networks offers a possible option to close this gap. Through a thorough investigation of various machine learning algorithms and their use in the context of medical time-series data, this research project takes a profound dive into the world of rural healthcare. The novel Long Short-Term Memory-Generative Adversarial Network (LSTM-GAN) architecture, which combines deep learning and generative modeling to enable predictive analytics in the medical domain, is at the center of this study.

Long-standing problems for rural healthcare systems include the lack of skilled medical professionals, restricted access to healthcare facilities, and the requirement for prompt diagnosis and treatment. With their ultra-low latency and tremendous bandwidth, 5G networks have created new opportunities for telemedicine and remote healthcare delivery that promise to ease some of these difficulties. However, in order to fully realize the benefits of 5G networks in rural healthcare, sophisticated machine learning algorithms are required to interpret the enormous volumes of real-time medical data.

In this study, we look at a lot of different things. First, we do a deep analysis of different machine learning algorithms, from standard statistical models to cutting-edge Machine learning techniques, to figure out their accuracy, precision, and recall for rural healthcare uses. We think about things like accuracy, how easy the data is to understand, and how efficiently it can be processed. We do this while keeping in mind that rural healthcare areas have limited resources.

Next, we talk about the LSTM-GAN design. This is a new way of doing things that combines the ability of Long Short-Term Memory (LSTM) networks to model sequences with the ability of Generative Adversarial Networks (GANs) to come up with new ideas. This hybrid architecture has the potential to not only correctly predict medical outcomes but also create fake data to fill in gaps in limited datasets. This is an important part of rural healthcare, where a lack of data often hurts the performance of models.

2. LITERATURE REVIEW

Medical Time-Series Analysis Over 5G Networks: Analysis of Various Rural Health Prediction Machine Learning Algorithms using an LSTM-GAN Architecture. A viable option for enhancing healthcare delivery in remote places is provided by the convergence of machine learning, sophisticated architectures like LSTM-GAN, and the developing 5G technology. The integration of 5G networks for medical time-series analysis, LSTM-GAN architecture, and machine learning in rural healthcare are all topics covered in this literature review.

Berlet et al. [11], digitization has an impact on contemporary life in many ways, including the growing availability of telemedicine apps and medical care options. Large bandwidths, low latency, and good quality of service in 5G mobile communication technology can fulfill the demands of this digitalized future, enabling wireless real-time data transmission in telemedical emergency health care applications. In order to enable mobile ultrasonography in preclinical diagnostics over 5G networks, the research creates and assesses a framework that is clinically appropriate for 5G usability assessments. The study discovered that the 5G network enabled two-way data connectivity between the ambulance and the distant hospital, enabling the transmission and reception of ultrasound and video camera data. This is one of the well-known success stories regarding the use of 5G in the medical industry. Numerous other research have looked at the usage of 5G networks for remote medical care.

Naruse et al. [12] investigated the precision of transmitting perinatal data, such as a cardiogram, using a test station outfitted with 5G transmission technology. The results showed that all data were sent with a delay of less than 1 second. The cardiogram waveform images did not lose any quality, and there were no transmission interruptions. Both the ultrasound scan and the video movie feeds appeared excellent.

According to Li et al. [13], there is an increasing need for robot-assisted laparoscopic telesurgery that is enabled by 5G in the field of urology; however, there is a dearth of convincing evidence that this is even possible, which calls for further research on the subject. According to the study's findings, combining surgical robots with 5G technology may present a viable new option for the telemedicine treatment of kidney cancers. Another study related to the use of 5G technology found that real-time remote gastrointestinal examinations over a 5G network are a useful and safe method for monitoring the stomach and small intestine Zhang[14]. A teleoperated surgery using a 5G network exhibited a smooth transition of tasks under the direction of a skilled surgeon [15]. Finally, Ahad et al. [16] have provided a thorough study of the state of 5G-enabled smart healthcare IoT technologies today and the key issues affecting their deployment.

Comparison of Above Review

| Author Name | Techniques | Findings |
|---------------------------|---|---|
| Berlet et al. [11] | 5G Usability Tests for Mobile Ultrasonography | 5G enables wireless real-time data transmission in telemedical emergency healthcare applications. |
| Naruse et al. [12] | Testing 5G for Perinatal Information Transfer | Perinatal information, including cardiocogram, can be transmitted with a delay of less than 1 second. |
| Li et al. [13] | 5G in Robot-Assisted Laparoscopic Telesurgery | 5G technology in tandem with surgical robots shows promise for treating kidney malignancies via telemedicine |
| Zhang et al. [14] | Real-Time Gastrointestinal Examinations | Remote gastrointestinal examinations using a 5G network are practical and secure for observing stomach and small bowel. |
| Wang et al. [15] | Teleoperated Surgery via 5G | Teleoperated surgery using a 5G network demonstrated seamless task flow under expert surgeon guidance. |
| Ahad et al. [16] | 5G-Enabled Smart Healthcare IoT Technologies | Provides an in-depth analysis of the current state of 5G-enabled smart healthcare IoT technologies. |

Manogaran et al. [17] proposed the MF-R and GC architectures for patient health monitoring. The proposed architecture consists of three phases: data collection, data transmission, and data storage. The &E system monitors blood pressure, heart rate, blood sugar, respiration rate, and body temperature. The CHDD dataset is used for this purpose and the stochastic gradient descent algorithm and logistic regression techniques are employed in the proposed smart system for detecting cardiac diseases. Vikas and Ananthula [18] designed a network, dubbed Body Sensor Network (BSN), for monitoring the health status of patients utilizing LabView software on the patient side. The proposed model enables physicians to remotely observe and monitor the health of their patients. Connecting the sensors used to collect patient health data to an Arduino board.

Luca et al. [19] created IoT-based and Smart Health Care System (SHS) architecture for monitoring patient health, tracking biomedical devices in hospitals, and tracking nursing staff in nursing institutes. IoT paradigms CoAP, REST, and 6LoWPAN are used to enable intercommunication and interoperation between SHS devices (i.e., UHF, WSN, and phones). The proposed system consists of two subsystems: one for patient monitoring and the other for handling medical emergencies. Loubet et al. [20] created a Cyber-physical system for monitoring the structural health of patients. The proposed architecture is developed using a smart mesh WSN comprised of sensing and communication nodes and a farfield Wireless Power Transmission system (a battery- and wire-free system). Wireless Power Transmission allows for the autonomous control of sensing nodes. Swati et al. [21] proposed a block-wise fine-tuning method for detecting brain lesions using a pretrained CNN model. The CE-MRI benchmark dataset is used for experimental analysis with an accuracy of 94.82%. Rahman et al. [22] proposed a Smart E-Health care system utilizing Fog Computing, thereby creating a geo-distributed intelligence layer between sensors and the cloud. Even implemented a smart health gateway

known as UT GATE and an Early Warning Score (EWS) health monitoring system to meet the challenges of energy efficiency, security, interoperability, reliability, mobility, and increased system intelligence.

Comparison of Above Reviews

| Author Name | Technique | Finding |
|---------------------------------|---|--|
| Manogaran et al. [17] | MF-R and GC Architectures for Health Monitoring | Proposed architecture includes data collection, transmission, and storage phases. - Monitors multiple health parameters, including blood pressure, heart rate, and blood sugar. - Uses CHDD dataset and employs stochastic gradient descent and logistic regression for cardiac disease detection. |
| Vikas and Ananthula [18] | Body Sensor Network (BSN) for Health Monitoring | Designed a BSN using LabView software for remote health monitoring. Utilizes Arduino board for sensor data collection. - Enables physicians to observe and monitor patients' health remotely. |
| Luca et al. [19] | IoT-Based Smart Healthcare System | Created an IoT-based Smart Health Care System architecture. - Enables patient health monitoring, biomedical device tracking, and staff tracking. - Uses IoT paradigms like CoAP, REST, and 6LoWPAN for intercommunication. |
| Loubet et al. [20] | Cyber-Physical System for Patient Health | Developed a cyber-physical system for monitoring patient health. - Utilizes smart mesh WSN with sensing and communication nodes. - Incorporates Wireless Power Transmission for autonomous sensing node control. |
| Swati et al. [21] | CNN Model for Brain Lesion Detection | Proposes a block-wise fine-tuning method for brain lesion detection. - Uses pretrained CNN models and the CE-MRI benchmark dataset. - Achieves an accuracy of 94.82% in experimental analysis. |
| Rahman et al. [22] | Smart E-Health Care System with Fog Computing | Implements a Smart E-Health care system with Fog Computing. - Introduces a geo-distributed intelligence layer (UT GATE) for improved system efficiency and intelligence. - Addresses challenges like energy efficiency, security, and reliability. Please note that the provided information summarizes the techniques and findings of each study. Specific details and results may vary, and the table provides a high-level overview of the key aspects of each study. |

3. RESEARCH METHODOLOGY

The goal of this research is to identify the component or components that have the greatest influence on spotting unusual behavior in elderly people, as well as the model that is most effective at spotting such components. The research primarily focuses on the social aspects of the implementation of 5G technology. This led to the selection of two different methodological approaches: the "Decision Making Trial and Evaluation Laboratory" (DEMATEL) for the purpose of identifying the element or factors that have the most influence on detecting the behavior of elderly people,

and the "Deep learning technique" as the model for the purpose of identifying the element or factors that have the most influence on detecting the behavior of elderly people.

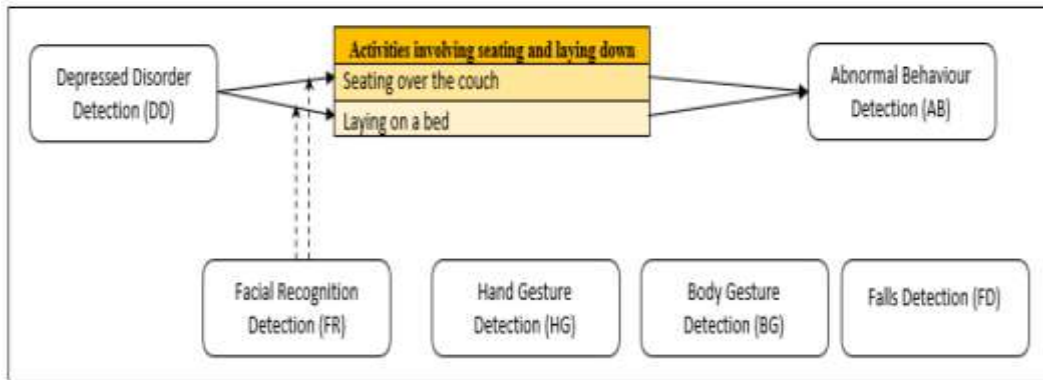


Figure 2: Conceptualized Elderly Walking at Home Activities Linked to the Elderly Behavior Dimension

In order to get the intended outcomes, both of these methods were used. While 5G technology would be seen as the quickest way to provide real-time network operations and deep learning would be seen as the strong technique to provide perfect prediction, the combination of these two approaches would allow for the development of a system that would assist elderly people in managing their affairs at home in a suitable manner. One reason for using these two strategies is due to this. Another argument in favor of the adoption of these two methods is the sequential sequencing of subjective and experimental evaluations, commencing with the subjective evaluations and ending with the use of deep learning.

- **DEMATEL Evaluation Tasks and Analytical Techniques:** There are a variety of methods available for determining what factors contributed to the occurrence of specific events within the activities of elderly people, which is necessary for identifying the crucial key criteria that influence an event or geriatric activities. The evaluation criteria and the analysis of the entire dataset of activities of elderly persons that was produced present a problem that must be resolved. In the event that 5G is adopted to monitor the day-to-day activities of elderly people in their homes, it will be necessary to extract the real cause and effect associated with a meaningful pattern for each "cause" of an activity and its corresponding "effect" for all of the typical activities involved and their causality. This will be completed in anticipation for the implementation of 5G. The technique ranks the various types and strengths of interactions between criteria to determine how the criteria influence one another, with the highest-ranked criterion assumed to be the cause criterion and the lower-ranked criterion the affected criterion. The subsequent steps constitute its application:

Step 1: Preparing expert opinion collection methods: This study uses a questioner based on the six criteria from Almutari et al. [23] and Alshammari et al. [24], which includes multiple preferences based on the Likert scale of inter scores: 0 = "No Influence," 1 = "Low Influence," 2 = "Medium Influence," 3 = "Extreme Influence," and 4 = "High Influence." The DEMATEL guidelines pick 15 sample subjects for this investigation. Unlike DEMATEL, which relies on expertise rather than statistics, the standard Structural Equation Modeling (SEM) approach requires a large sample size to show causal relationships between components.

Participants' assessments of each criterion's influence are shown by the number x_{ij} , where the cause-and-effect standards are denoted by i and j , respectively. An $n \times n$ non-negative direct relation matrix is formed by equation 1 for each participant's response, which is given as $n = 1, 2, 3, \dots, n$.

$$x^y = \begin{bmatrix} x_{ij}^y \end{bmatrix}_{n \times n} \quad (1)$$

where y represents the number of participation of each participant with $1 \leq y \leq q$ as a result the equation generate matrix q for x^1, x^2, \dots, x^q where q is the number of participants. Furthermore, the average aggregated decision matrix for all the participants $Z = z_{ij}$ is presented by equation 2:

$$z_{ij} = \frac{1}{q} \sum_{i=1}^q x_{ij}^y \quad (2)$$

Step 2: Creating the normalized direct relation matrix: Equation 3 produces the normalized direct relation matrix D as follows:

$$D = \max \left(\sum_{j=1}^n z_{ij}, \sum_{i=1}^n z_{ij} \right) \quad (3)$$

Because of this, each cell in matrix Z will ultimately have a value that falls inside the range [0, 1].

Step 3: Construct the total relation matrix: by raising the normalized initial direct-relation matrix D to the power of m, where m is indirect influence D^m , we obtain the total relation matrix T, which represents the total influence generated by the participant's response. Since the total relation is the sum of $D^1 + D^2 + \dots + D^m$ hence D^m , will converge to zero, we know that the total relation matrix T is equal to the original direct-relation matrix D, then the total relation matrix $T = D^1 + D^2 + \dots + D^m$ is $T = D^1 + D^2 + D^3 \dots + D^m = D(I - D)^{-1}$ thus

$$T = D(I - D)^{-1} \quad (4)$$

where I is an $n \times n$ identity matrix.

Step 4: Create a cause-and-effect relationship diagram by following these steps: The results arrived at as a result of the calculations performed in the previous steps will act as the basis on which the relationship diagram will be constructed. As a result, the cause-and-effect relationship has been depicted for each combination of coordinates that makes up the sum of the rows and columns. The interactions between the criteria are depicted in these rows and columns, and they include details that help determine which criteria are most crucial as well as how the criteria affect one another.

- **Deep Learning for Unusual Behavior Detection of Elderly People At Home:** The "classification problem" includes the identification of odd behavior among older people when they are at home. This is because the method uses a time series as a model to forecast future values using values or qualities that have already been observed. For this reason, DEMATEL was utilized to thoroughly extract the attribute/values necessary for learning how to spot anomalous behavior in older persons when they are at home. Long Short-Term Memory (LSTM) recurrent neural networks, which have memory and can learn any temporal dependence between observations, as well as the CNN model, which has convolutional hidden layers that operate over a one-dimensional sequence, are adopted for the fact that all of them are able to learn any temporal dependence between observations when taking into account the theoretical and practical implications of deep learning models.
- **The Convolutional Neural Network Architecture:** The Convolutional Neural Network (CNN) is the most well-known deep learning method, according to this study. It is a subset of neural networks that are frequently used to analyze images in three dimensions, specifically the height, breadth, and depth. It also applies to the classification of objects. The current study intends to use CNNs to detect the attributes associated to the activities of elderly people in determining their unusual behavior because they can learn directly from the raw time series data, extract features from sequences of observations, and require neither domain expertise nor manually engineered input characteristics.

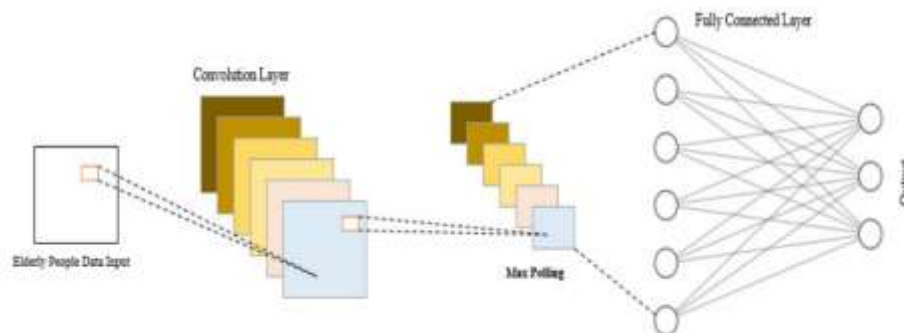


Figure 3: Conceptualized Elderly Activities involving Walking at home Associated to Elderly Behavior Dimension.

Six layers, including input, convolution, activation, pooling, completely linked, and output, make up the CNN's overall working procedures. This study used a two-stage CNN methodology. The feature extractor, a software program that can automatically extract features from raw data, is used in the research as a starting point. A fully connected network serving as the second option can be trained to conduct classification utilizing the first step's newly acquired features. The convolution layer, activation layer, pooling layer, and fully connected layer of a convolutional neural network (CNN) are built in this study using a feature extractor. As input and output, these layers require feature maps (see Figure 3). "Fitting" the model to the training data after it has been created allows it to be used to make predictions.

- **Evaluation Performance Metrics for the Deep Learning Algorithm:** Deep learning's effectiveness must be evaluated. To assess how well it performs, performance metrics are employed. Various performance measures

show various facets of the model's operation. It shows how an algorithm or technique performs in comparison to the norm. Accuracy, precision, and recall are the performance metrics used to contrast the two deep learning-based models (CNN and LSTM) for effectiveness. From the confusion matrix below, all the measurements are derived:

TP is “true positive” FP is “false positive”, TN is “true negative”, and FN is “false negative”. Thus accuracy, precision and recall are derived by equations 5, 6 and 7, respectively.

$$\text{Accuracy: } \frac{TP + TN}{TP + TN + FP + FN} \quad (5)$$

$$\text{Precision: } \frac{TP}{TP + FP} \quad (6)$$

$$\text{Recall: } \frac{TP}{TP + FN} \quad (7)$$

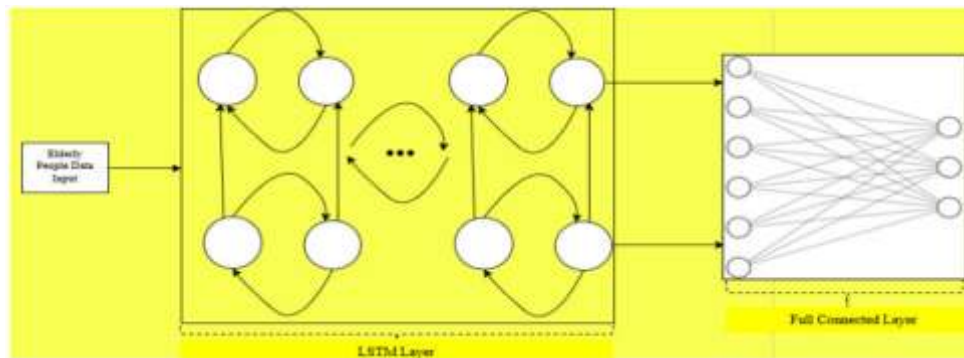


Figure 4: Conceptualized Elderly Activities involving Walking at home Associated to Elderly Behavior Dimension.

4. RESULT

4.1 DEMATEL Experimental Analysis

The DEMATEL technique has been used to analyze the important factors that affect 5G adoption for identifying odd behaviors in senior persons. The process of getting the results of the analysis begins with coding the criteria and entering the data into an MS Excel sheet: "Abnormal Behavior Detection (AB)," "Falls Detection (FD)," "Hand Gesture Detection (HG)," "Facial Recognition Detection (FR)," "Depressed Disorder Detection (DD)," and "Body Gesture Detection (BG)."

| | | | | | | | | | | | | | | | | | | | | | | |
|------|----|----|----|----|----|----|----|----|----|----|----|----|----|----|----|----|----|----|----|----|---|---|
| | AB | FD | HG | FR | DD | BG | | AB | FD | HG | FR | DD | BG | | AB | FD | HG | FR | DD | BG | | |
| ex1 | AB | 0 | 2 | 3 | 4 | 2 | 2 | AB | 0 | 4 | 3 | 3 | 2 | 3 | AB | 0 | 2 | 3 | 4 | 3 | 4 | |
| | FD | 2 | 0 | 4 | 3 | 3 | 4 | FD | 4 | 0 | 3 | 3 | 3 | 3 | FD | 2 | 0 | 3 | 2 | 3 | 3 | |
| | HG | 3 | 3 | 0 | 3 | 4 | 2 | HG | 3 | 2 | 0 | 3 | 3 | 2 | HG | 2 | 2 | 0 | 2 | 3 | 2 | |
| | FR | 3 | 3 | 4 | 0 | 3 | 4 | FR | 4 | 2 | 3 | 0 | 4 | 3 | FR | 4 | 2 | 2 | 0 | 3 | 4 | |
| | DD | 1 | 2 | 4 | 2 | 0 | 3 | DD | 2 | 3 | 3 | 3 | 0 | 3 | DD | 3 | 4 | 3 | 2 | 0 | 3 | |
| BG | 2 | 3 | 2 | 3 | 2 | 0 | BG | 4 | 2 | 2 | 3 | 2 | 0 | BG | 3 | 2 | 2 | 3 | 2 | 0 | 0 | |
| ex4 | AB | 0 | 4 | 3 | 3 | 3 | 2 | AB | 0 | 3 | 2 | 2 | 2 | 3 | AB | 0 | 2 | 3 | 2 | 2 | 2 | 4 |
| | FD | 2 | 0 | 3 | 2 | 3 | 4 | FD | 3 | 0 | 2 | 4 | 2 | 4 | FD | 2 | 0 | 2 | 2 | 2 | 2 | 3 |
| | HG | 3 | 3 | 0 | 3 | 3 | 2 | HG | 3 | 2 | 0 | 2 | 2 | 3 | HG | 2 | 2 | 0 | 2 | 2 | 2 | 4 |
| | FR | 2 | 2 | 3 | 0 | 2 | 4 | FR | 4 | 4 | 2 | 0 | 2 | 3 | FR | 2 | 2 | 2 | 0 | 2 | 2 | 3 |
| | DD | 3 | 4 | 3 | 3 | 0 | 4 | DD | 2 | 2 | 2 | 2 | 0 | 2 | DD | 3 | 2 | 3 | 2 | 0 | 2 | 3 |
| BG | 3 | 4 | 3 | 4 | 3 | 0 | BG | 3 | 3 | 3 | 4 | 4 | 0 | BG | 4 | 3 | 3 | 2 | 4 | 0 | 0 | |
| ex7 | AB | 0 | 3 | 2 | 2 | 1 | 4 | AB | 0 | 2 | 3 | 4 | 3 | 3 | AB | 0 | 4 | 3 | 2 | 4 | 3 | 3 |
| | FD | 3 | 0 | 2 | 2 | 1 | 3 | FD | 2 | 0 | 3 | 4 | 3 | 2 | FD | 2 | 0 | 3 | 4 | 4 | 2 | 2 |
| | HG | 3 | 2 | 0 | 2 | 2 | 3 | HG | 2 | 3 | 0 | 2 | 3 | 3 | HG | 3 | 3 | 0 | 3 | 3 | 3 | 4 |
| | FR | 2 | 2 | 3 | 0 | 1 | 4 | FR | 4 | 4 | 4 | 0 | 3 | 2 | FR | 2 | 4 | 3 | 0 | 4 | 2 | 2 |
| | DD | 1 | 1 | 2 | 2 | 0 | 4 | DD | 3 | 3 | 3 | 3 | 0 | 2 | DD | 4 | 4 | 3 | 2 | 0 | 4 | 0 |
| BG | 4 | 2 | 3 | 2 | 3 | 0 | BG | 2 | 2 | 2 | 4 | 2 | 0 | BG | 2 | 2 | 3 | 3 | 4 | 0 | 0 | |
| ex10 | AB | 0 | 2 | 3 | 2 | 4 | 3 | AB | 0 | 2 | 3 | 2 | 3 | 4 | AB | 0 | 3 | 2 | 3 | 3 | 3 | 4 |
| | FD | 2 | 0 | 2 | 3 | 3 | 4 | FD | 2 | 0 | 3 | 2 | 3 | 4 | FD | 3 | 0 | 3 | 2 | 3 | 3 | 3 |
| | HG | 2 | 2 | 0 | 2 | 2 | 4 | HG | 4 | 3 | 0 | 3 | 3 | 2 | HG | 3 | 3 | 0 | 3 | 3 | 2 | 2 |
| | FR | 2 | 3 | 2 | 0 | 3 | 2 | FR | 2 | 2 | 3 | 0 | 4 | 3 | FR | 3 | 2 | 3 | 0 | 4 | 4 | 4 |
| | DD | 2 | 3 | 2 | 3 | 0 | 3 | DD | 3 | 3 | 3 | 4 | 0 | 3 | DD | 3 | 4 | 3 | 4 | 0 | 3 | 3 |
| BG | 3 | 4 | 4 | 2 | 2 | 0 | BG | 2 | 4 | 2 | 2 | 3 | 0 | BG | 4 | 3 | 2 | 2 | 2 | 0 | 0 | |
| ex13 | AB | 0 | 2 | 4 | 3 | 3 | 3 | AB | 0 | 3 | 2 | 4 | 2 | 3 | AB | 0 | 3 | 2 | 3 | 2 | 3 | 3 |
| | FD | 2 | 0 | 3 | 2 | 4 | 3 | FD | 3 | 0 | 3 | 3 | 3 | 3 | FD | 3 | 0 | 2 | 3 | 3 | 4 | 4 |
| | HG | 2 | 3 | 0 | 3 | 3 | 4 | HG | 4 | 3 | 0 | 3 | 3 | 2 | HG | 2 | 2 | 0 | 2 | 3 | 3 | 3 |
| | FR | 3 | 2 | 3 | 0 | 4 | 2 | FR | 4 | 3 | 2 | 0 | 2 | 3 | FR | 4 | 3 | 2 | 0 | 2 | 4 | 4 |
| | DD | 2 | 3 | 3 | 4 | 0 | 3 | DD | 2 | 3 | 3 | 2 | 0 | 3 | DD | 2 | 2 | 3 | 2 | 0 | 2 | 2 |
| BG | 3 | 3 | 4 | 2 | 3 | 0 | BG | 4 | 3 | 2 | 2 | 2 | 0 | BG | 2 | 4 | 3 | 2 | 3 | 0 | 0 | |

As a result, the thoughts of the fifteen experts who contributed to the study in the form of Likert scale integer scores of 0, 1, 2, 3, and 4 are compiled into an initial individual matrix and presented in a nn non-negative direct relation matrix using equation 1, as shown in the equation at the bottom of the previous page. The average aggregate of the participant's decision matrices—also known as the direct impact matrix—is determined using Equation 2. Below is a presentation of the computation's findings:

$$Z = \begin{matrix} 0.0000 & 2.7333 & 2.7333 & 2.8667 & 2.6000 & 3.2000 \\ 2.4667 & 0.0000 & 2.7333 & 2.7333 & 2.8667 & 3.2667 \\ 2.7333 & 2.5333 & 0.0000 & 2.5333 & 2.8000 & 2.8000 \\ 3.0000 & 2.6667 & 2.7333 & 0.0000 & 2.8667 & 3.1333 \\ 2.4000 & 2.8667 & 2.8667 & 2.6667 & 0.0000 & 3.0000 \\ 3.0000 & 2.9333 & 2.6667 & 2.6667 & 2.7333 & 0.0000 \end{matrix}$$

After that, the direct influence matrix was normalized using equation 3, and the result is displayed in the following matrix:

$$D = \begin{matrix} 0.0000 & 0.1775 & 0.1775 & 0.1861 & 0.1688 & 0.2078 \\ 0.1602 & 0.0000 & 0.1775 & 0.1775 & 0.1861 & 0.2121 \\ 0.1775 & 0.1645 & 0.0000 & 0.1645 & 0.1818 & 0.1818 \\ 0.1948 & 0.1732 & 0.1775 & 0.0000 & 0.1861 & 0.2035 \\ 0.1558 & 0.1861 & 0.1861 & 0.1732 & 0.0000 & 0.1948 \\ 0.1948 & 0.1905 & 0.1732 & 0.1732 & 0.1775 & 0.0000 \end{matrix}$$

The normalized initial direct-relation matrix is used to calculate the total relation matrix, which represents the total influence brought about by the participant's response. This equation is shown in the equation at the bottom of the page.

One can determine the causes and effects based on the analysis by adding the sums of the rows and columns of the matrix that makes up the total relation matrix, or the rows matrix vectors and columns matrix vectors. By resolving equations 5 and 6, we may determine these. In other words, if the vectors r and c reflect the sum of the rows and the sum of the columns of the entire relation matrix, the "cause" and "effect" can be identified.

Table 1: Direct influenced of the criteria among themselves

| | ri | ci | ri+ci | ri-ci | identity |
|--|----|----|-------|-------|----------|
| | | | | | |

| | | | | | |
|-----------|--------|---------|---------|---------|--------|
| AB | 0.6714 | 1.5706 | 2.2419 | -0.8993 | effect |
| FD | 0.6497 | 1.4792 | 2.1289 | -0.8296 | effect |
| H | 0.6962 | 1.4763 | 2.1724 | -0.7803 | effect |
| FR | 0.7114 | 1.4872 | 2.1985 | -0.7759 | effect |
| DD | 0.6868 | -2.7453 | -2.0587 | 3.4319 | effect |
| BG | 1.5293 | 1.6764 | 3.2056 | -0.1472 | effect |

The determined outcome is thus shown in the matrix above. As stated in section IV step 4, the final assessment confirms the causal relationship between the cause and the effect. In light of this, only DD was determined to belong to the cause group (see Table 1), indicating that it had an impact on the other criteria. The remaining criteria, however, were determined to belong to the effect group, indicating that they were impacted by the other criteria.

The threshold's value is thus determined using equation 7. As a result, the estimated threshold value equals 0.1373, indicating that the relationships diagram is affected by any value in the total relation matrix that is higher than the threshold value. As a result, the values in question are highlighted in bold in the matrix below:

| | | | | | | | | | | | |
|---------------------------------|---------|---------|---------|---------|---------|---------------------------------|---------------|---------------|---------------|----------------|---------------|
| <i>I (Identity Matrix)</i> | | | | | | <i>D(Normalized Matrix)</i> | | | | | |
| 1 | 0 | 0 | 0 | 0 | 0 | 0.0000 | 0.1775 | 0.1775 | 0.1861 | 0.1688 | 0.2078 |
| 0 | 1 | 0 | 0 | 0 | 0 | 0.1602 | 0.0000 | 0.1775 | 0.1775 | 0.1861 | 0.2121 |
| 0 | 0 | 1 | 0 | 0 | 0 | 0.1775 | 0.1645 | 0.0000 | 0.1645 | 0.1818 | 0.1818 |
| 0 | 0 | 0 | 1 | 0 | 0 | 0.1948 | 0.1732 | 0.1775 | 0.0000 | 0.1861 | 0.2035 |
| 0 | 0 | 0 | 0 | 1 | 0 | 0.1558 | 0.1861 | 0.1861 | 0.1732 | 0.0000 | 0.1948 |
| 0 | 0 | 0 | 0 | 0 | 1 | 0.1948 | 0.1905 | 0.1732 | 0.1732 | 0.1775 | 0.0000 |
| <i>I-D</i> | | | | | | <i>Inverse(I-D)</i> | | | | | |
| 1.0000 | -0.1775 | -0.1775 | -0.1861 | -0.1688 | -0.2078 | 1.1145 | 0.2479 | 0.2473 | 0.2581 | -0.4838 | 0.2874 |
| -0.1602 | 1.0000 | -0.1775 | -0.1775 | -0.1861 | -0.2121 | 0.2491 | 1.0940 | 0.2441 | 0.2485 | -0.4728 | 0.2867 |
| -0.1775 | -0.1645 | 1.0000 | -0.1645 | -0.1818 | -0.1818 | 0.2677 | 0.2424 | 1.1007 | 0.2461 | -0.4336 | 0.2728 |
| -0.1948 | -0.1732 | -0.1775 | 1.0000 | -0.1861 | -0.2035 | 0.2836 | 0.2508 | 0.2534 | 1.1072 | -0.4746 | 0.2910 |
| -0.1558 | -0.1861 | -0.1861 | -0.1732 | 1.0000 | -0.1948 | 0.2511 | 0.2565 | 0.2561 | 0.2508 | 0.3917 | 0.2805 |
| -0.1948 | -0.1905 | -0.1732 | -0.1732 | 2.8225 | 1.0000 | -0.3486 | -0.3818 | -0.3936 | -0.3759 | -1.4473 | 0.4166 |
| <i>T(Total relation matrix)</i> | | | | | | <i>T(Total relation matrix)</i> | | | | | |
| 0.1145 | 0.2479 | 0.2473 | 0.2581 | -0.4838 | 0.2874 | 0.1145 | 0.2479 | 0.2473 | 0.2581 | -0.4838 | 0.2874 |
| 0.2491 | 0.0940 | 0.2441 | 0.2485 | -0.4728 | 0.2867 | 0.2491 | 0.0940 | 0.2441 | 0.2485 | -0.4728 | 0.2867 |
| 0.2677 | 0.2424 | 0.1007 | 0.2461 | -0.4336 | 0.2728 | 0.2677 | 0.2424 | 0.1007 | 0.2461 | -0.4336 | 0.2728 |
| 0.2836 | 0.2508 | 0.2534 | 0.1072 | -0.4746 | 0.2910 | 0.2836 | 0.2508 | 0.2534 | 0.1072 | -0.4746 | 0.2910 |
| 0.2511 | 0.2565 | 0.2561 | 0.2508 | -0.6083 | 0.2805 | 0.2511 | 0.2565 | 0.2561 | 0.2508 | -0.6083 | 0.2805 |
| 0.4046 | 0.3876 | 0.3746 | 0.3765 | -0.2721 | 0.2580 | 0.4046 | 0.3876 | 0.3746 | 0.3765 | -0.2721 | 0.2580 |
| <i>Sum(cj)</i> | | | | | | <i>Sum(rj)</i> | | | | | |
| | | | | | | 1.5705 | 1.4791 | 1.4762 | 1.4871 | -2.7452 | 1.6763 |

To illustrate how the impact can link the criteria in Table 2, arrows are drawn from the first criterion in each row to the criteria whose values are greater than the threshold value.

Table 2: The values of the relationships impact.

| | | | | | | |
|-----------|---------------|---------------|---------------|---------------|----------------|---------------|
| | AB | FD | HG | FR | DD | BG |
| AB | 0.1146 | 0.2480 | 0.2474 | 0.2582 | -0.4839 | 0.2875 |
| FD | 0.2490 | 0.0941 | 0.2442 | 0.2486 | -0.4729 | 0.2868 |
| HG | 0.2678 | 0.2425 | 0.1008 | 0.2462 | -0.4337 | 0.2729 |
| FR | 0.2837 | 0.2509 | 0.2535 | 0.1073 | -0.4747 | 0.2911 |
| DD | 0.2512 | 0.2566 | 0.2562 | 0.2509 | -0.6084 | 0.2806 |

| | | | | | | |
|----|--------|--------|--------|--------|---------|--------|
| BG | 0.4047 | 0.3877 | 0.3766 | 0.3766 | -0.2722 | 0.2581 |
|----|--------|--------|--------|--------|---------|--------|

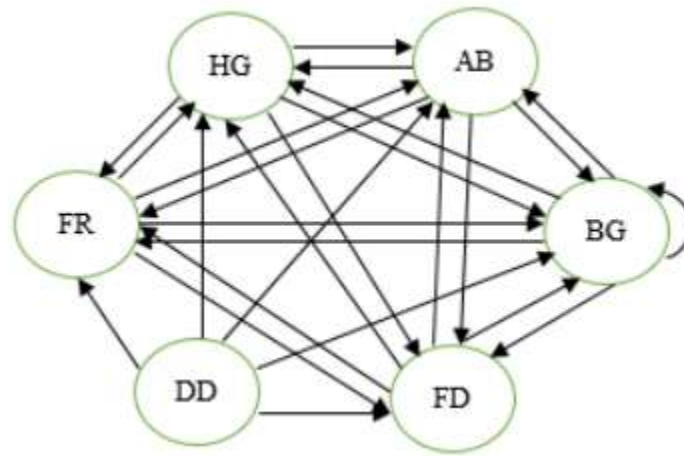


Figure 5: The Interrelationship Diagram

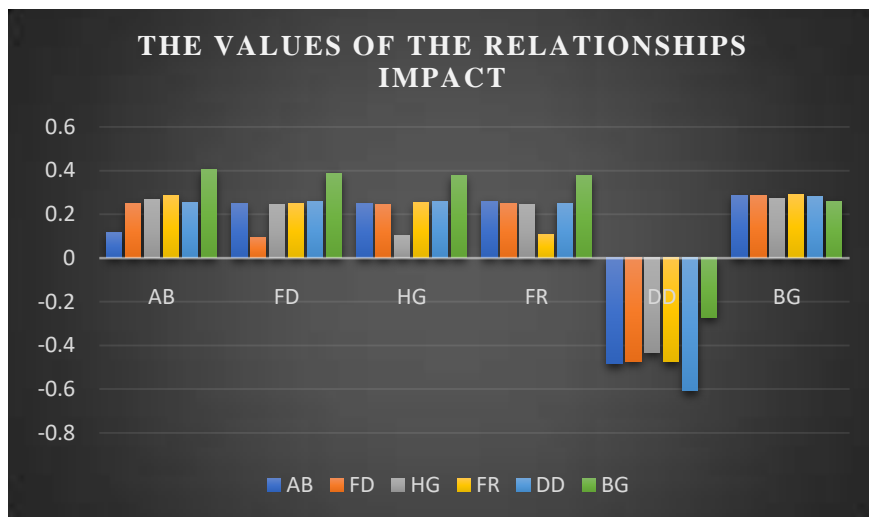


Figure 6: Graphical Representation

This is intended to demonstrate how the effect binds the attribute together. Figure 6 depicts the resultant diagrams derived from this analysis.

According to the findings of DEMATEL analysis, the "depressive disorder" is the key component that contributes to atypical behavior in elderly individuals. This conclusion was obtained based on the research findings. On the other hand, the effects of odd behavior in older individuals are observable in terms of all other variables. According to the findings of this study, "depressive disorder" has no effect on any of the other characteristics associated with this topic.

4.2 Dataset for the Analysis

Alshammari et al.'s SIMulated Activities of Daily Living (SIMADL) dataset was obtained using OpenSHS, an open-source simulation platform, which allowed the generation of residents' data for classification of Activities of Daily Living. With the assistance of OpenSHS, the research was able to utilize the simulated datasets containing 29 columns of binary data representing sensor results for on (1) and off (0) (see Figure 5 for a snapshot of the dataset). Seven individuals enacted a typical day at the office, at home, in the morning, and in the evening. 84 files were created, which is roughly equivalent to 63 days of labor. Each participant contributed six files to the generation of a total of forty-two datasets, of which twenty-four were used to simulate Activities of Daily Living classification problems using the classification dataset and the remaining twenty-four were used to simulate anomaly detection problems using the anomaly detection dataset. Throughout the simulation, participants classified their own actions. Personal, Sleep, Eat, Recreation, Work, Other, and Anomaly were among the adjectives employed by the individuals.

Table 3

| | | | | | | | | | | | | | | | | | | | | | | | | | | | | | | | | | | | | |
|---|----------|----|------|-------------|----------------|------------|------------|--------|--------------|----------|-------------|------------|--------------|-----------------|-------------|-------------|--------------|--------|-------|--------------|-----------------|-------------|-------------|--------------|-----|---------------|------------------|--------------|--------------|-------------|--------------|---|---|---|---|---|
| 1 | wardrobe | tv | oven | officeLight | officeDoorLock | officeDoor | officeCarp | office | mainDoorLock | mainDoor | livingLight | livingCarp | kitchenLight | kitchenDoorLock | kitchenDoor | kitchenCarp | hallwayLight | fridge | couch | bedroomLight | bedroomDoorLock | bedroomDoor | bedroomCarp | bedTableLamp | bed | bathroomLight | bathroomDoorLock | bathroomDoor | bathroomCarp | bedroomCarp | bedTableLamp | | | | | |
| 2 | 0 | 0 | 0 | 0 | 0 | 0 | 0 | 0 | 0 | 0 | 0 | 0 | 0 | 0 | 0 | 0 | 0 | 0 | 0 | 0 | 0 | 0 | 0 | 0 | 0 | 0 | 0 | 0 | 0 | 0 | 0 | 0 | 0 | | | |
| 3 | 0 | 0 | 0 | 0 | 0 | 0 | 0 | 0 | 0 | 0 | 0 | 0 | 0 | 0 | 0 | 0 | 0 | 0 | 0 | 0 | 0 | 0 | 0 | 0 | 0 | 0 | 0 | 0 | 0 | 0 | 0 | 0 | 0 | 0 | | |
| 4 | 0 | 0 | 0 | 0 | 0 | 0 | 0 | 0 | 0 | 0 | 0 | 0 | 0 | 0 | 0 | 0 | 0 | 0 | 0 | 0 | 0 | 0 | 0 | 0 | 0 | 0 | 0 | 0 | 0 | 0 | 0 | 0 | 0 | 0 | 0 | |
| 5 | 0 | 0 | 0 | 0 | 0 | 0 | 0 | 0 | 0 | 0 | 0 | 0 | 0 | 0 | 0 | 0 | 0 | 0 | 0 | 0 | 0 | 0 | 0 | 0 | 0 | 0 | 0 | 0 | 0 | 0 | 0 | 0 | 0 | 0 | 0 | 0 |
| 6 | 0 | 0 | 0 | 0 | 0 | 0 | 0 | 0 | 0 | 0 | 0 | 0 | 0 | 0 | 0 | 0 | 0 | 0 | 0 | 0 | 0 | 0 | 0 | 0 | 0 | 0 | 0 | 0 | 0 | 0 | 0 | 0 | 0 | 0 | 0 | 0 |
| 7 | 0 | 0 | 0 | 0 | 0 | 0 | 0 | 0 | 0 | 0 | 0 | 0 | 0 | 0 | 0 | 0 | 0 | 0 | 0 | 0 | 0 | 0 | 0 | 0 | 0 | 0 | 0 | 0 | 0 | 0 | 0 | 0 | 0 | 0 | 0 | 0 |

Table 3 provides a summary of the outcomes of each methodology and dataset; there are numerous intriguing aspects to these outcomes. In this study, the researchers analyze the objective through the lens of anomaly detection, where the nature of the captured anomaly varies across models. For LSTM to achieve its objective of identifying sequences of abnormal tempo rally behavior, it must integrate memory cells that can store temporal dependency and information. As indicated in the "Introduction" section, deep learning can acquire a hierarchical feature representation directly from the raw data.

Table 4

| Technique | Accuracy | Precision | Recall |
|-----------|----------|-----------|--------|
| LSTM-GAN | 97% | 95% | 95% |
| CNN | 91% | 90% | 90% |

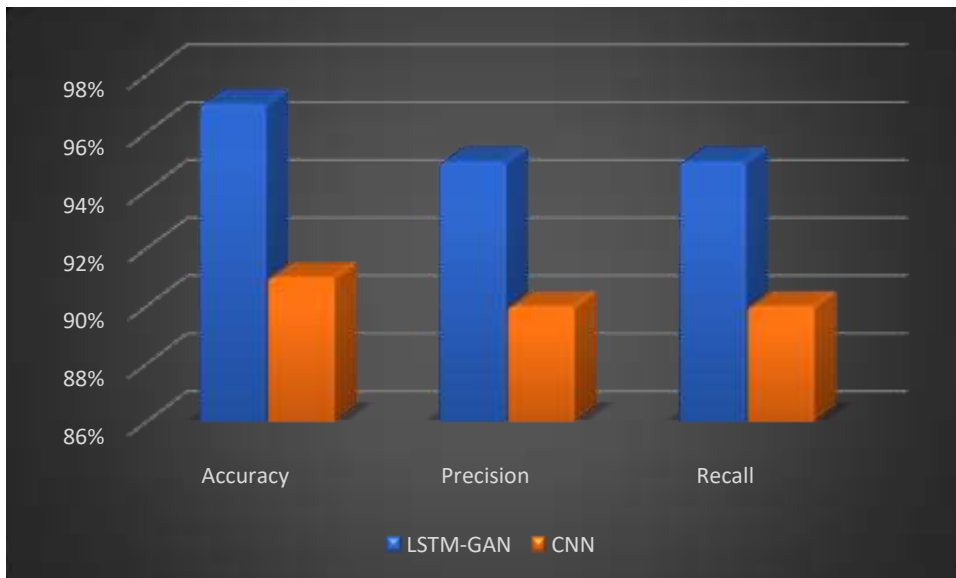


Figure 7: Graphical Representation

It is crystal clear that the LSTM model is superior to temporal information identification and prediction. The LSTM-GAN model effectively captures the fundamental traits required to increase the detection accuracy of aberrant behavior, according to the metrics shown in Table 5. With a 97% accuracy rate, LSTM-GAN performs at a high level. The CNN models were able to reach a 91% accuracy rate. The model was found to have the best performance in terms of rare identification based on the data obtained in terms of accuracy, precision, and recall.

CONCLUSION

In conclusion, the integration of LSTM-GAN architecture, 5G networks, and machine learning algorithms is a game-changing development for improving rural healthcare. In order to improve healthcare services in underserved rural communities, this research aims to give a thorough roadmap for the use of these technologies in the context of medical time-series analysis. Ageing abnormalities may be found using 5G networks and deep learning techniques. Using more sophisticated algorithms and data sets, 5G networks are able to train and recognize in real time. Additionally, 5G makes it easier to process geriatric in-home monitoring data in real time. The method must, however, take into account the elderly's most important factors because they face more challenging settings and living conditions. In order to analyze the most crucial criterion (feature) for creating a model to detect anomalous behavior in the elderly, this study advocated using the "Decision Making Trial and Evaluation Laboratory" (DEMATEL).

Based on a study using the DEMATEL criteria, we applied CNNs and LSTMs to identify unusual senior behavior. The technique models used to identify the most crucial factor in identifying geriatric behavior were the "Decision Making Trial and Evaluation Laboratory" (DEMATEL) and the "Deep Learning Technique" (DLT). Using the DEMATEL and DLT, we determined the most significant behavioral characteristics of aged people. Utilize 5G technology and deep learning to enable real-time network operations. Another reason to employ these two approaches when developing a home management system for seniors is to combine subjective and experimental evaluations in a step-by-step evolution from subjective evaluations to the deep learning implementation technique of perfect prediction. This encourages the two approaches to study. The Simulated Activities of Daily Living (SIMADL) dataset and the behavior of elderly persons were analyzed using CNN and LSTM. The LSTM outperforms earlier methods at ageing anomaly detection with 97% accuracy.

REFERENCES

- [1]. Alwan, A. (2011). Global status report on noncommunicable diseases 2010. World Health Organization.
- [2]. Rashid, S. & Razak, S. A. (2019). Big data challenges in 5G networks. In 2019 Eleventh international conference on ubiquitous and future networks (ICUFN), Zagreb, Croatia, pp. 152–157. <https://doi.org/10.1109/ICUFN.2019.8806076>
- [3]. G. B. Mohammad, S. Shitharth, S. A. Syed et al., "Mechanism of internet of things (IoT) integrated with radio frequency identification (RFID) technology for healthcare system," *Mathematical Problems in Engineering*, vol. 2022, pages, Article ID 4167700, 2022.
- [4]. D. H. Prasad and M. Srikanth, "Mobile healthcare monitoring system in mobile cloud computing," *Int J Comput Technol Appl*, vol. 6, no. 1, pp. 43–46, 2015
- [5]. F. Serpush, M. B. Menhaj, B. Masoumi, and B. Karasfi, "Wearable sensor-based human activity recognition in the smart healthcare system," *Computational Intelligence and Neuroscience*, vol. 2022, Article ID 1391906, 31 pages, 2022.
- [6]. Sravan Kumar Pala, "Detecting and Preventing Fraud in Banking with Data Analytics tools like SASAML, Shell Scripting and Data Integration Studio", *IJBMV*, vol. 2, no. 2, pp. 34–40, Aug. 2019. Available: <https://ijbmv.com/index.php/home/article/view/61>
- [7]. U. Ahmad, H. Song, A. Bilal, S. Saleem, and A. Ullah, "Securing insulin pump system using deep learning and gesture recognition," in *Proceedings of the IEEE International Conference On Trust, Security And Privacy In Computing And Communications/12th IEEE International Conference On Big Data Science And Engineering (TrustCom/BigDataSE)*, New York, NY, USA, August 2018.
- [8]. Amol Kulkarni, "Amazon Redshift: Performance Tuning and Optimization," *International Journal of Computer Trends and Technology*, vol. 71, no. 2, pp. 40-44, 2023. Crossref, <https://doi.org/10.14445/22312803/IJCTT-V71I2P107>
- [9]. S. Tuli, N. Basumatary, S. S. Gill et al., "HealthFog: an ensemble deep learning based smart healthcare system for automatic diagnosis of heart diseases in integrated IoT and fog computing environments," *Future Generation Computer Systems*, vol. 104, pp. 187–200, 2020.
- [10]. Sravan Kumar Pala, "Advance Analytics for Reporting and Creating Dashboards with Tools like SSIS, Visual Analytics and Tableau", *IJOPE*, vol. 5, no. 2, pp. 34–39, Jul. 2017. Available: <https://ijope.com/index.php/home/article/view/109>
- [11]. T. Ahmad and H. Chen, "A review on machine learning forecasting growth trends and their real-time applications in different energy systems," *Sustainable Cities and Society*, vol. 54, Article ID 102010, 2020.
- [12]. S. Shitharth, G. B. Mohammad, and K. Sangeetha, "Predicting epidemic outbreaks using IOT, artificial intelligence and cloud," in *Fusion of Internet of ;ings, Artificial Intelligence, and Cloud Computing in Health Care*, pp. 197–222, Springer, Berlin, Germany, 2021
- [13]. M. Berlet, T. Vogel, M. Gharba, J. Eichinger, E. Schulz, H. Friess, D. Wilhelm, D. Ostler, and M. Kranzfelder, "Emergency telemedicine mobile ultrasounds using a 5G-enabled application: Development and usability study," *JMIR Formative Res.*, vol. 6, no. 5, May 2022, Art. no. e36824.

- [14]. K. Naruse, T. Yamashita, Y. Onishi, Y. Niitaka, F. Uchida, K. Kawahata, M. Ishihara, and H. Kobayashi, "High-quality transmission of cardiocogram and fetal information using a 5G system: Pilot experiment," *JMIR Med. Informat.*, vol. 8, no. 9, Sep. 2020, Art. no. e19744.
- [15]. J. Li et al., "Application of improved robot-assisted laparoscopic telesurgery with 5G technology in urology," *Eur. Urol.*, vol. 83, no. 1, pp. 41–44, Jan. 2023.
- [16]. T. Zhang, Y. Chen, X. Jiang, C. He, J. Pan, W. Zhou, J. Hu, Z. Liao, and Z. Li, "5G-based remote magnetically controlled capsule endoscopy for examination of the stomach and small bowel," *United Eur. Gastroenterol. J.*, vol. 11, no. 1, pp. 42–50, Feb. 2023.
- [17]. W. Wang, Z. Wang, H. Gong, L. Jin, and F. Wei, "5G-assisted remote guidance in laparoscopic simulation training based on 3D printed dry lab models," *Indian J. Surg.*, pp. 1–5, Oct. 2022.
- [18]. Amol Kulkarni, "Amazon Athena: Serverless Architecture and Troubleshooting," *International Journal of Computer Trends and Technology*, vol. 71, no. 5, pp. 57-61, 2023. Crossref, <https://doi.org/10.14445/22312803/IJCTT-V71I5P110>
- [19]. Sravan Kumar Pala, "Implementing Master Data Management on Healthcare Data Tools Like (Data Flux, MDM Informatica and Python)", *IJTD*, vol. 10, no. 1, pp. 35–41, Jun. 2023. Available: <https://internationaljournals.org/index.php/ijtd/article/view/53>
- [20]. V. Vikas and S. Ananthula, "Internet of things (IoT) based smart health care system," in *Proceedings of the International Conference on signal processing, communication, power and embedded system (SCOPE5)*, Odisha, India, October 2016.
- [21]. C. Luca, D. D. Donno, L. Mainetti et al., "An IoT-aware architecture for smart healthcare systems," vol. 2, no. 6, pp. 515–526, 2015.
- [22]. G. Loubet, A. Takacs, and D. Dragomirescu, "Implementation of a battery-free wireless sensor for cyber-physical systems dedicated to structural health monitoring applications," *IEEE Access*, vol. 7, pp. 24679–24690, 2019.
- [23]. Sravan Kumar Pala, "Synthesis, characterization and wound healing imitation of Fe₃O₄ magnetic nanoparticle grafted by natural products", *Texas A&M University - Kingsville ProQuest Dissertations Publishing*, 2014. 1572860.
- [24]. Z. N. K. Swati, Q. Zhao, M. Kabir et al., "Brain tumor classification for MR images using transfer learning and finetuning," *Computerized Medical Imaging and Graphics*, vol. 75, pp. 34–46, 2019.
- [25]. M. M. Rahman, D. R. Dipta, and M. M. Hasan, "Dynamic time warping assisted SVM classifier for Bangla speech recognition," in *Proceedings of the International Conference on Computer, Communication, Chemical, Material and Electronic Engineering (IC4ME2)*, Rajshahi, Bangladesh, November 2018.
- [26]. M. Almutairi, L. A. Gabralla, S. Abubakar, and H. Chiroma, "Detecting elderly behaviors based on deep learning for healthcare: Recent advances, methods, real-world applications and challenges," *IEEE Access*, vol. 10, pp. 69802–69821, 2022.
- [27]. T. Alshammari, N. Alshammari, M. Sedky, and C. Howard, "SIMADL: Simulated activities of daily living dataset," *Data*, vol. 3, no. 2, p. 11, Apr. 2018.